Scientific Research Publishing

Thermodynamic Properties of CaCl₂-CaF₂-CaO System: Phase Diagram Investigation

Julien Claquesin[1,2], Mathieu Gibilaro[1]*, Laurent Massot[1], Olivier Lemoine[2], Gilles Bourges[2], Pierre Chamelot[1]

[1]Laboratoire de Génie Chimique UMR 5503 UPS-CNRS-INP, Université de Toulouse, Toulouse, France
[2]CEA, DAM, VALDUC, Is-sur-Tille, France
Email: *gibilaro@chimie.ups-tlse.fr

Abstract

The CaCl₂-CaF₂-CaO phase diagram was investigated in the CaO low region (<40 mol.%). CaCl₂-CaF₂ and CaCl₂-CaO binary diagrams, constituting the ternary system, were first studied by Differential Scanning Calorimetry (DSC) measurements and X-Ray Diffraction (XRD) characterization; a good agreement was obtained between the phase diagram models calculated with Fact-Sage® software (FTsalt database) and present experimental data. As the CaF₂-CaO liquidus could not be measured by DSC due to the high melting temperature, this diagram was calculated using FTsalt database combined with FToxid database of FactSage® software. The ternary phase diagram was obtained by calculations and exhibits an eutectic at the composition CaCl₂-CaF₂-CaO (78.2-15.7-6.1 mol.%) melting at 637°C, and five peritectic points. Measurements of relevant vertical cross-sections for three CaCl₂-CaF₂ compositions (50-50, 40-60 and 30-70 mol.%) up to 18 mol.% CaO are in agreement with the ternary phase diagram model. For each section, the liquidus temperature is constant up to around 11 mol.% CaO and then sharply increases. Moreover, an increase of CaF₂ content in CaCl₂-CaF₂ melt leads to a decrease of the CaO solubility in isothermal condition.

Keywords

1. Introduction

CaCl₂-rich corner of the CaCl₂-CaF₂-CaO phase diagram, up to 50 mol.% CaF₂ and 20 mol.% CaO, was investigated by Wenz *et al.* [1]. These authors showed

the existence of:

- a ternary eutectic point at the composition $CaCl_2$-CaF_2-CaO (79-17-4 mol.%) melting at 625°C,
- two peritectic points at the composition $CaCl_2$-CaF_2-CaO (67-23-10 mol.%) and (64-23-13 mol.%) melting respectively at 660°C and 670°C.

CaF_2-rich part (>50 mol.% CaF_2) of the phase diagram is still unknown and needs to be investigated. To build it, binary phase diagrams constituting the ternary system, $CaCl_2$-CaF_2, $CaCl_2$-CaO and CaF_2-CaO, must be previously considered.

The $CaCl_2$-CaF_2 system was investigated by several authors [1]-[6]:

- in the $CaCl_2$-rich region, they all suggested a single eutectics in the composition range 18.5 - 25 mol.% CaF_2 at around 650°C as well as a peritectic point at 735°C around 41 mol.% CaF_2,
- the system exhibits CaFCl compound at 50 mol.% CaF_2 which is known to have an incongruent melting point [7]. In the composition range 41-50 mol.% CaF_2, this phase changes to α-CaF_2 at around 735°C,
- the liquidus data are more scattered in the CaF_2-rich part (>50 mol.% CaF_2).

Moreover, some of these results were obtained by visual-polythermal method which is not very accurate according to Chartrand *et al.* [8]. These authors proposed a calculated phase diagram using a modified quasi-chemical model, and confirmed it with data from several studies.

The $CaCl_2$-CaO system was only investigated in the $CaCl_2$-rich part and data were compiled by Shaw *et al.* [1] [9] [10] [11] [12]:

- the system exhibits an eutectic point in the 5 - 6.5 mol.% CaO composition range at around 750°C. However, a different eutectic composition was found by Threadgill [13] (28.7 mol.% CaO and 593°C),
- a second eutectic was proposed by Neumann *et al.* [10] at 21 mol.% and 800°C. These authors also reported the $CaO(CaCl_2)_4$ compound at 20 mol.% CaO, which melts congruently at 839°C. Similar results were obtained by Perry *et al.* [11] specifying that the 20 - 22 mol.% CaO region may exhibit a peritectic point instead of eutectic point. However, Wenz *et al.* [1] did not report it: they proposed a peritectic point at 18.5 mol.% melting at 835°C and suggested the $CaO(CaCl_2)_2$ compound at 33 mol.% CaO which was considered in Shaw *et al.* study [12],
- a sharp increase of the liquidus temperature for higher CaO amount above 22 mol.% was reported by all the authors [1] [10] [11] [14] [15],
- Neumann *et al.* [10] noticed a thermal plateau at 703°C on the cooling curve, attributed to the $CaO(CaCl_2)_4$ allotropic phase transformation.

The liquidus values are very dispersed since finely colloidal suspension of CaO can be obtained, resulting that it is not completely solubilized according to Freidina *et al.* [14].

The liquidus temperatures of the CaF_2-CaO phase diagram are higher than 1300°C as the melting points of both pure CaF_2 and CaO compounds are 1418°C

and 2572˚C respectively [16]:

- in the literature, authors [17]-[25] indicated a single eutectic shape diagram, determined by calculations and experimental measurements. There is no consensus about an accurate eutectic point composition which varies in the 15 - 28 mol.% CaO range and the solidus temperature is around 1360˚C according to Zaitsev *et al.* *[19]* and Kim *et al.* [20],

- no specific compound was identified in the diagram, but partial CaO solubility in solid CaF_2 phase was reported by Kim *et al.* [20] with a maximum around 5 mol.% CaO at the solidus temperature. This author also identified the CaF_2 allotropic transition $\alpha \rightarrow \beta$ at 1146˚C without any effect on the CaO solubility,

- Baak [26] proposed a two-liquid phase region in the 0.8 - 10 mol.% CaO composition range, up to 1485˚C.

According to the literature, discrepancies exist on the binary phase diagrams constituting the $CaCl_2$-CaF_2-CaO ternary system. In this study, both $CaCl_2$-CaF_2 and $CaCl_2$-CaO systems were investigated by combining experimental data and modeling. From these results, the ternary phase diagram was calculated and vertical cross-sections measurements were then performed to verify the model.

2. Experimental

Differential Scanning Calorimetry (DSC) technique was used to measure solidus, liquidus and phase transition temperatures of mixtures. Experiments were carried out in a heat-flux DSC MHTC 96 from SETARAM. The calorimeter is a 3D quasi-Calvet type sensor and can measures up to 1400˚C. The standard deviation was estimated from three runs with each calibration metals (Sn: T°_{fus} = 231.9˚C, Pb: T°_{fus} = 327.5˚C, Sb: T°_{fus} = 630.6˚C, Ag: T°_{fus} = 961.8˚C, Au: T°_{fus} = 1064.2˚C, Cu: T°_{fus} = 1084.6˚C) and salts ($CaCl_2$: T°_{fus} = 772˚C, LiF: T°_{fus} = 848˚C) and is lower than 1˚C. From measurements, a correlation among the measured heat flow and the corresponding molar enthalpy was found. Boron nitride crucibles were used for chloro-fluoride samples and graphite crucibles for CaO-base system.

Calcium chloride (Alfa Aesar 99.99%), calcium fluoride (Alfa Aesar 99.99 %) and calcium oxide (Alfa Aesar 99.95%) were used. The CaO was previously heated up to 900˚C under vacuum ($\approx 10^{-1}$ mbar) for 12 hours to remove the residual water. Samples were prepared in a glove box under argon atmosphere by mixing the pure chemicals and around 150 mg were analysed. They were heat-treated into the apparatus under vacuum (400˚C, $\approx 10^{-2}$ mbar). Then, a pre-melting step was carried out under argon to ensure a good mixing of the chemicals. DSC analyses were performed under argon flow (30 mL·min^{-1}) with a heating rate of 2˚C min^{-1}. No mass loss was observed during the experiment.

Crystallographic phases were identified by X-Ray Diffraction analysis (XRD) with a Bruker D4-ENDEAVOR diffractometer. Patterns were recorded from 20˚ to 70˚ by 0.016˚ step (2θ) in the Bragg-Brentano geometry using the Kα radia-

tion of the copper anode (40 kV, 40 mA). Samples were prepared in a glove box under inert argon atmosphere: the salt was protected by a Kapton film to prevent water absorption.

Binary and ternary phase diagrams modeling was performed using Phase Diagram module from FactSage® 6.3 software [27] [28]. In the Phase Diagram module, the Gibbs energy minimization is used for calculations where axis and constant parameters can be set, such as the volume, the temperature, the pressure… In this study, FTsalt and FToxid databases were used and the pressure was fixed to 1 atmosphere.

3. Results and Discussion

3.1. Binary Diagrams

3.1.1. CaCl$_2$-CaF$_2$ System

A classical DSC-signal from a binary sample of CaCl$_2$-CaF$_2$ (70-30 mol.%) is shown in **Figure 1** and exhibits a sharp endothermic peak at around 660°C, solidus—followed by a second broad endothermic peak at around 710°C, liquidus—typical of a binary mixture. The solidus temperature was measured as onset point whereas liquidus temperature at the peak maximum, as recommended by Höhne *et al.* [29]. The values were reported on the diagram in **Figure 2** and are consistent with other authors [1]-[6] and FactSage® model (FTsalt database).

Eutectic composition could not be accurately determined on DSC curves since the peaks are not well defined in the 15 - 23 mol.% CaF$_2$ composition range. The determination of the eutectic composition was done by using of a Tamman diagram [30] [31] [32], representing the molar enthalpy associated to a first-order phase transition versus the molar fraction, based on the lever rule application. The resulting diagram has a triangle shape and the baseline endpoints indicate specific compositions (eutectics, peritectics, stoichiometric compound, solid solubility…).

In this case, the Tamman plot was established using enthalpy in the 5 - 40 mol.% CaF$_2$ composition range. Both left and right endpoints from the baseline
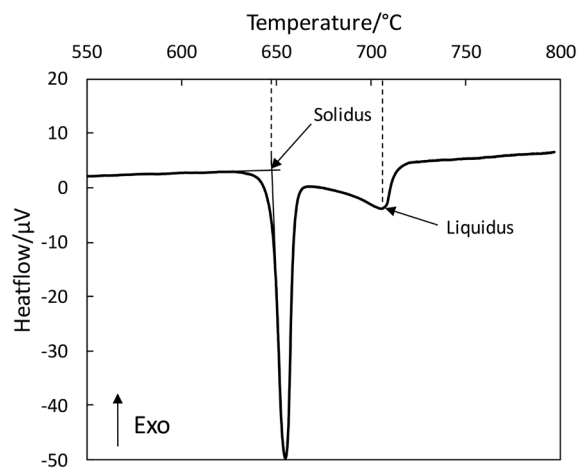

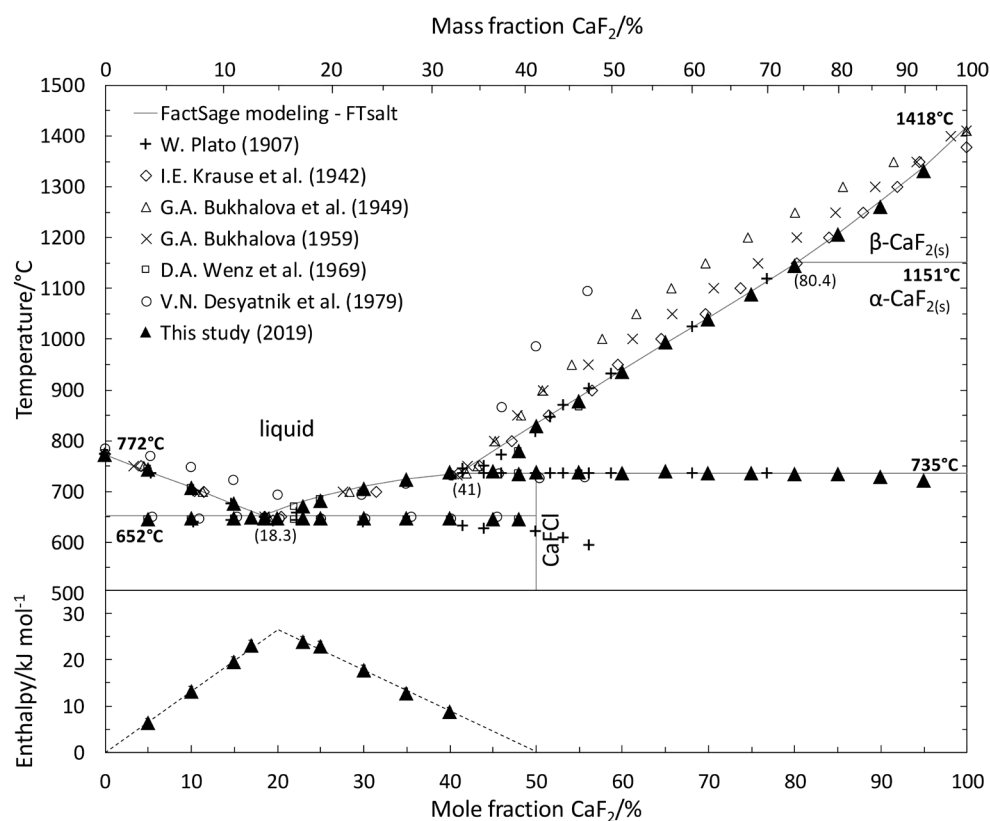**Figure 1.** Classical DSC curve of a CaCl$_2$-CaF$_2$ (70-30 mol.%) sample at 2°C·min^{-1}.

Figure 2. Phase diagram (upper part) and Tamman diagram (lower part) of the CaCl₂-CaF₂ system.

are close to 0 and 50 mol.% CaF₂ respectively, indicating a negligible solid solubility into CaCl₂ and the presence of CaFCl stoichiometric compound. The highest point indicates the eutectic composition, 20.0 mol.% CaF₂ at 647°C, close to the calculated one (18.3 mol.% CaF₂ and 652°C) in agreement with the model.

To confirm the presence of the CaFCl stoichiometric compound, a melted mixture of CaCl₂-CaF₂ (40-60 mol.%) annealed for 72 hours at 650°C was prepared for phases identification by XRD analysis. The resulting pattern is shown in **Figure 3** where CaFCl was identified, which is consistent with the model and the literature data [7]. As it was expected for this composition, α-CaF₂ was also detected without any segregation.

Unexpected signal occurred in the CaF₂-rich part at around 647°C and was not observed in the data available in the literature: it could be attributed to a segregation effect. One way to avoid it is to introduce an annealing step after the salt pre-melting: this procedure was successful as no more unexpected signal was observed.

3.1.2. CaCl₂-CaO System

The CaCl₂-CaO diagram was investigated in the 0 - 27 mol.% CaO composition range. Measured data are reported in the diagram of **Figure 4** and are coherent with the FactSage® model (FTsalt database).

The eutectic composition was determined by a Tamman diagram using solidus enthalpy in the 1 - 17 mol.% CaO composition range at 750°C. Due to the
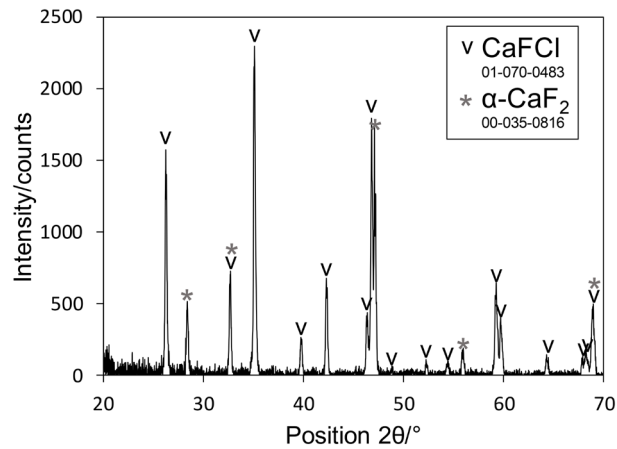
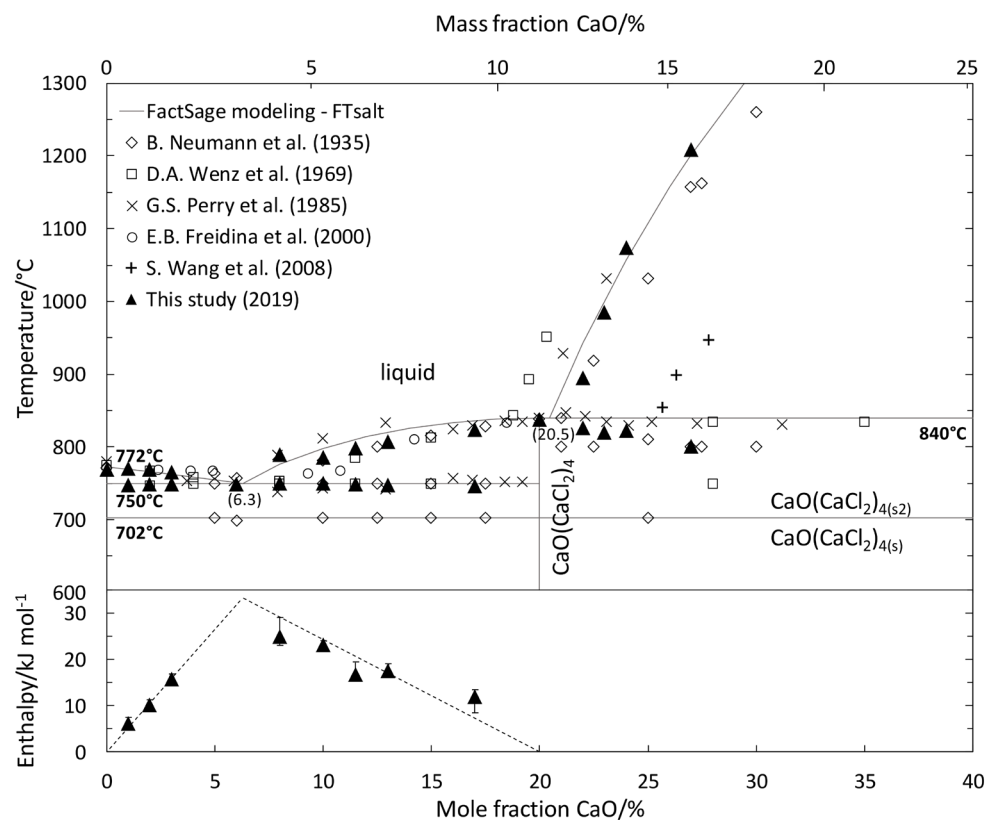**Figure 3.** XRD pattern of CaCl₂-CaF₂ (40-60 mol.%) sample.

Figure 4. Phase diagram (upper part) and Tamman diagram (lower part) of the CaCl₂-CaO system.

triangle sides trend, hypothesis was made that solid solubility is negligible in pure CaCl₂, and that stoichiometric compound exists at 20 mol.% CaO. It permitted to set the Tamman baseline endpoints at 0 and 20 mol.% CaO; the determined eutectic composition is then 6.3 mol.% CaO and is in agreement with the calculated value within the model and consistent with the literature [1] [10] [11] [14].

The presence of a second eutectic point at around 21 mol.% CaO mentioned by Neumann *et al.* [10] could not be clearly identified since the interval composition

is extremely narrow. However, the abrupt increase of the liquidus temperature is observed at higher CaO contents: the temperature rises from 900°C at 22 mol.% CaO up to 1200°C at 27 mol.% CaO, which is consistent with other studies [10] [11] but a 2 mol.% difference can be noted with Wenz *et al.* work [1] and even more with Wang *et al.* data [15] (4 mol.%).

Furthermore, the extrapolated curve reaches around 32 mol.% of CaO at 1400°C and is in agreement with the CaO solubility value determined by Sano *et al.* [33].

To prove the existence of a stoichiometric compound in the binary system, a mixture of $CaCl_2$ containing 13 mol.% of CaO was melted and annealed for 48 hours at 650°C. It was then characterized by XRD for phase identification. The pattern is shown in **Figure 5** and reveals the presence of $CaCl_2$ and $CaO(CaCl_2)_4$ compound, confirming the endpoint composition of the Tamman triangle basis (20 mol.% CaO), as well as the presence of three peaks that could not be attributed.

A slight endothermic peak is observed at around 715°C for every samples similarly to the thermal plateau observed by Neumann *et al.* [10] at 703°C on the cooling curves; this signal can be attributed to the allotropic phase transition of $CaO(CaCl_2)_4$ compound.

3.1.3. CaF₂-CaO System

Due to the high liquidus temperature (>1300°C), the CaF_2-CaO system was not investigated by DSC. However, the phase diagram was calculated using FTsalt database which offers satisfying models for both $CaCl_2$-CaF_2 and $CaCl_2$-CaO systems. The model was improved by including additional CaF_2/CaO data from FToxid database and was plotted in **Figure 6**; it exhibits an eutectic point at 19.8 mol.% CaO melting at 1305°C, and the CaO solubility domain into α- and β-CaF_2 solids mentioned in Kim *et al.* study [20].

3.2. The Ternary Diagram

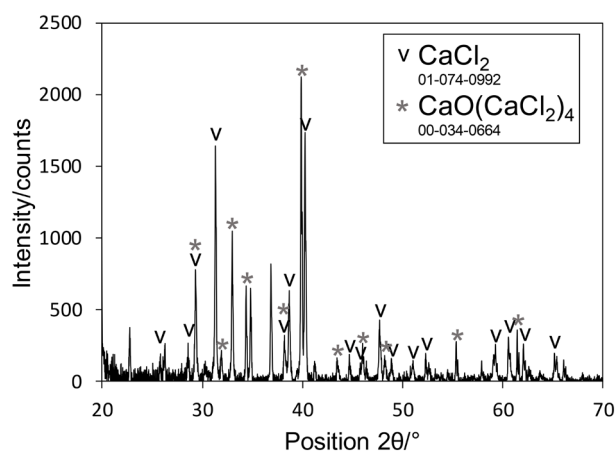To build the $CaCl_2$-CaF_2-CaO diagram, the three binary diagrams constituting

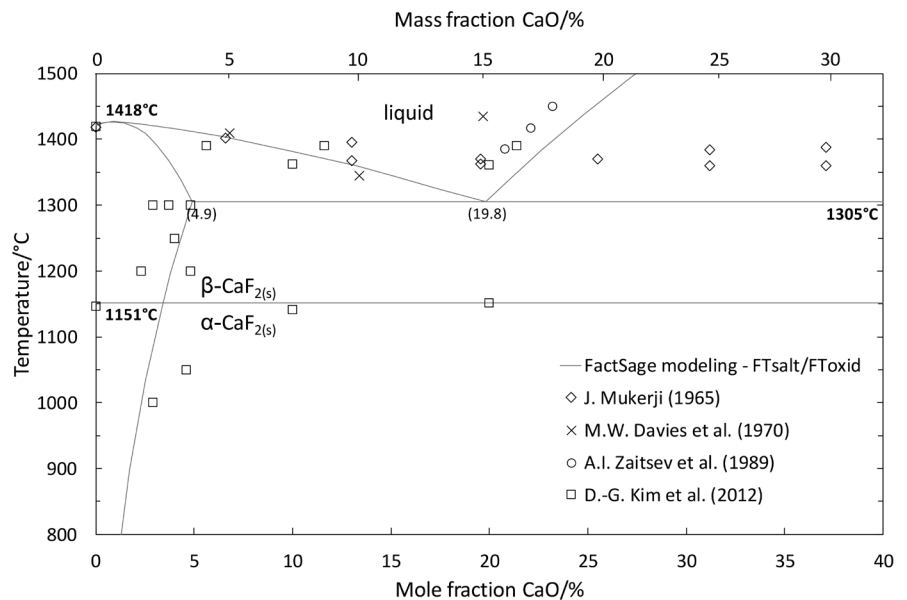**Figure 5.** XRD pattern of $CaCl_2$-CaO (87-13 mol.%) sample.

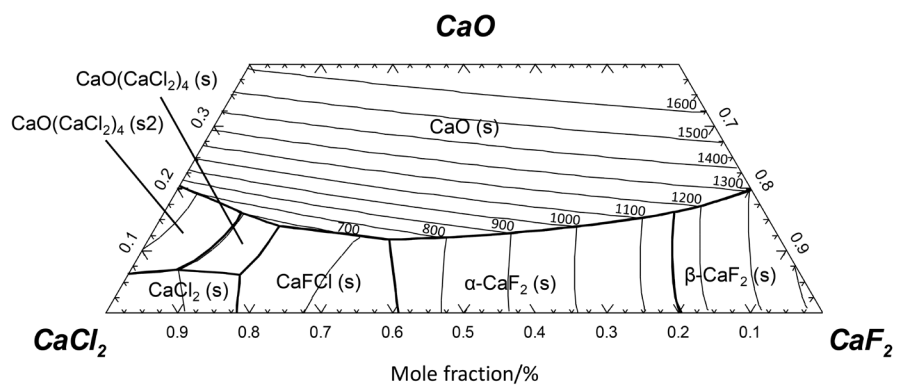**Figure 6.** Calculated phase diagram of the CaF_2-CaO system.

Figure 7. $CaCl_2$-CaF_2-CaO phase diagram calculated with FactSage®.

the system were used. The calculated ternary phase diagram is plotted in **Figure 7** and exhibits an eutectic point at the composition $CaCl_2$-CaF_2-CaO (78.2-15.7-6.1 mol.%) melting at 637°C, similar as in Wenz *et al.* diagram [1]. However, four peritectic points are identified in the $CaCl_2$-rich region and another one in the CaF_2-rich region contrary to Wenz *et al.* work [1] who identified only two peritectic points in the $CaCl_2$-rich region; characteristics of specific intersection points are summarized in **Table 1**.

Three vertical liquidus cross-sections were investigated by DSC; a $CaCl_2$-CaF_2 composition (50-50, 40-60 and 30-70 mol.%) was set and the CaO amount was increased up to 18 mol.%. Measurements for richer CaF_2 and CaO concentrations were not possible due to the temperature limitation of the apparatus.

The results are shown in **Figure 8** and the following observations can be noticed:

- the general shape of the liquidus temperature is in agreement with the model for each cross-section: a plateau from 0 to a threshold composition around 11 mol.% CaO and then a sharp increase,

Table 1. Liquidus temperature and composition of invariant points.

Invariant point	Liquidus T°/°C	Mole fraction/%		
		CaCl₂	CaF₂	CaO
Eutectics	637	78.2	15.7	6.1
Peritectics	650	68.8	17.3	13.9
Peritectics	702	86.7	6.4	6.9
Peritectics	702	73.0	10.9	16.1
Peritectics	709	54.6	33.7	11.7
Peritectics	1151	12.5	71.4	16.1
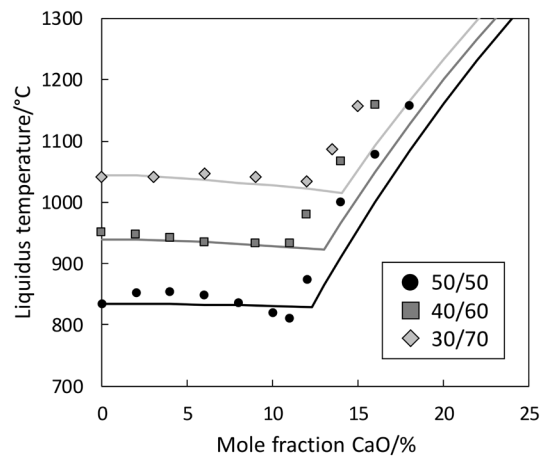
Figure 8. Liquidus cross-sections of the CaCl₂-CaF₂-CaO phase diagram (solid lines correspond to the model).
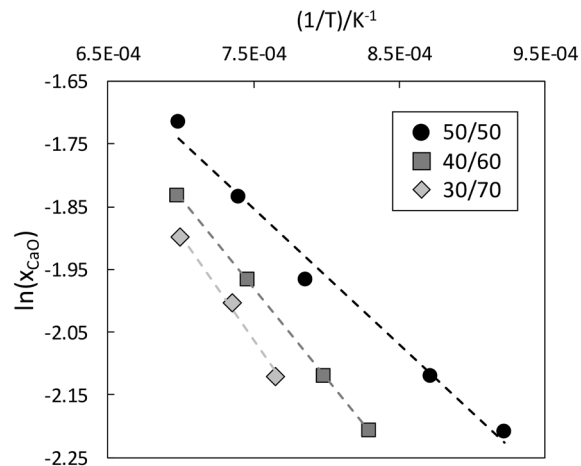
Figure 9. Evolution of the CaO solubility logarithm vs. the inverse of the absolute temperature.

- a slight difference of the threshold composition between measurements and the model, which could be attributed to the data selected to calculate the CaF₂-CaO phase diagram and was not experimentally verified.

At constant temperature, the CaO solubility decreases when the CaF₂ portion

in the melt increases, as observed at 1400°C by Sano *et al.* [33] in the investigated area. To compare his data with the present work, the logarithm of CaO solubility (x_{CaO}) above 11 mol.% was plotted as a function of the inverse of the absolute temperature in Figure 9. A linear relationship was obtained for all compositions and equations were extrapolated toward 1400°C to determine the CaO solubility; data are reported in Table 2.

Table 2. Linear regression equation of the CaO solubility logarithm vs. inverse of the absolute temperature and CaO solubility values at 1400°C

Molar fraction of CaCl₂-CaF₂/%	Equation	CaO solubility extrapolated at 1400°C/mol.%	CaO solubility [33]/mol.%
50-50	$\ln(x_{CaO}) = \dfrac{-2166.2}{T(K)} - 0.2273$	21.8	26.0
40-60	$\ln(x_{CaO}) = \dfrac{-2861.9}{T(K)} + 0.1671$	21.4	24.0
30-70	$\ln(x_{CaO}) = \dfrac{-3378.8}{T(K)} + 0.4709$	21.3	23.0

The CaO solubility calculated at 1400°C is slightly different than the ones determined by Sano *et al.* [33] with a maximum discrepancy reaching 4.2 mol.% in the equimolar CaCl₂-CaF₂ medium. However, the CaO solubility evolution is similar with a decrease of the solubilized CaO amount while the CaCl₂ is replaced by CaF₂ at constant temperature (1400°C).

4. Conclusions

In this work, binaries CaF₂-CaO, CaCl₂-CaF₂, CaCl₂-CaO and ternary CaCl₂-CaF₂-CaO phase diagrams system were investigated in the CaO low region (<40 mol.% CaO) by thermal analysis (DSC) and thermodynamic calculations (FactSage®-FTsalt/FToxid databases).

The ternary diagram exhibits an eutectic point in the CaCl₂-rich region at 637°C, CaCl₂-CaF₂-CaO (78.2-15.7-6.1 mol.%), and five peritectic points. Vertical cross-sections analysis was performed in three CaCl₂-CaF₂ compositions (50-50, 40-60 and 30-70 mol.%) up to 18 mol.% CaO. Each section exhibits the same shape: a plateau up to around 11 mol.% CaO and then a rapid increase of the liquidus temperature. The measurements show that CaO solubility decreases while CaCl₂ is replaced by CaF₂ in this diagram region.

Acknowledgements

Conflicts of Interest

The authors declare no conflicts of interest regarding the publication of this paper.

References

[1] Wenz, D.A., Johnson, I. and Wolson, R.D. (1969) CaCl$_2$-Rich Region of the CaCl$_2$-CaF$_2$-CaO System. *Journal of Chemical & Engineering Data*, **14**, 250-252. https://doi.org/10.1021/je60041a027

[2] Krause, I.E. and Bergman, A.G. (1942) Singular Irreversible-Reciprocal Systems without Separation into Layers from Potassium and Calcium and Calcium Chlorides and Fluorides, and Sodium and Calcium Chlorides and Fluorides. *Doklady Akademii Nauk SSSR*, **35**, 20-24.

[3] Bukhalova, G.A. (1959) The Ternary Resiprocal System Formed by Fluorides and Chlorides of Sodium and Calcium. *Russian Journal of Inorganic Chemistry*, **4**, 47-49.

[4] Bukhalova, G.A. and Bergman, A.G. (1949) Troinaya vzaimnaya sistema iz ftoridov i khloridov litiya i kaltsiya. *Doklady Akademii Nauk SSSR*, **66**, 67-70.

[5] Plato, W. (1907) Erstarrungserscheinungen an anorganischen Salzen und Salzgemischen II. *Zeitschrift für Physikalische Chemie*, **58**, 350-372. https://doi.org/10.1515/zpch-1907-5814

[6] Desyatnik, V.N., Kurbatov, N.N., Strelov, V.A. and Shchavelevc, V.V. (1979) Melting Point Diagrams of Systems Containing Potassium and Calcium Fluoride. *Izv Vysshikh Uchebnykh Zaved Tsvetnaya Metall*, **4**, 65-68.

[7] Messer, C.E. (1970) Hydrides versus Fluorides: Structural Comparisons. *Journal of Solid State Chemistry*, **2**, 144-155. https://doi.org/10.1016/0022-4596(70)90062-9

[8] Chartrand, P. and Pelton, A.D. (2001) Thermodynamic Evaluation and Optimization of the Li, Na, K, Mg, Ca/F, Cl Reciprocal System Using the Modified Quasi-Chemical Model. *Metallurgical and Materials Transactions A*, **32**, 1417-1430. https://doi.org/10.1007/s11661-001-0231-6

[9] Arndt, K. and Loewenstein, W. (1909) Über Lösungen von Kalk und Kieselsäure in geschmolzenem Chlorcalcium. *Zeitschrift für Elektrochemie und angewandte physikalische Chemie*, **15**, 784-790.

[10] Neumann, B., Kröger, C. and Jüttner, H. (1935) Die Systeme Erdalkalichlorid-Erdalkalioxyd und die Zersetzung der Erdalkalichloride durch Wasserdampf. *Zeitschrift für Elektrochemie und angewandte physikalische Chemie*, **41**, 725-736.

[11] Perry, G.S. and Macdonald, L.G. (1985) Role of CaCl$_2$ in the Reduction of PuO$_2$. *Journal of Nuclear Materials*, **130**, 234-241. https://doi.org/10.1016/0022-3115(85)90312-5

[12] Shaw, S. and Watson, R. (2009) Solubility of Calcium in CaCl$_2$-CaO. *ECS Transactions*, **16**, 301-308. https://doi.org/10.1149/1.3159334

[13] Threadgill, W.D. (1965) The Calcium Chloride-Calcium Oxide Fused Salt Electrolytic System: Solubilities, Metal Contents, and Freezing Points. *Journal of The Electrochemical Society*, **112**, 632-633. https://doi.org/10.1149/1.2423626

[14] Freidina, E.B. and Fray, D.J. (2000) Study of the Ternary System CaCl$_2$-NaCl-CaO by DSC. *Thermochimica Acta*, **356**, 97-100. https://doi.org/10.1016/S0040-6031(00)00454-8

[15] Wang, S., Zhang, F., Liu, X. and Zhang, L. (2008) CaO Solubility and Activity Coefficient in Molten Salts CaCl$_{2-x}$ (x=0, NaCl, KCl, SrCl2, BaCl2 and LiCl). *Thermochimica Acta*, **470**, 105-107. https://doi.org/10.1016/j.tca.2008.02.007

[16] Patnaik, P. (2003) Handbook of Inorganic Chemicals. Vol. 529, McGraw-Hill, New York.

[17] Seo, W.-G., Zhou, D. and Tsukihashi, F. (2005) Calculation of Thermodynamic Properties and Phase Diagrams for the CaO-CaF$_2$, BaO-CaO and BaO-CaF$_2$ Systems by Molecular Dynamics Simulation. *Materials Transactions*, **46**, 643-650. https://doi.org/10.2320/matertrans.46.643

[18] Seo, W.-G., Zhou, D., Hamano, T. and Tsukihashi, F. (2004) Calulation of Phase Diagrams for the CaO-CaF$_2$ and CaO-BaO Binary Systems by Using Molecular Dynamics. *7th International Conference on Molten Slags Fluxes and Salts*, Cape Town, 25-28 January 2004, 835-838.

[19] Zaitsev, A.I., Zemchenko, M.A., Litvina, A.D. and Mogutnov, B.M. (1993) Thermodynamic Calculation of Phase Equilibria in the CaF$_2$-SiO$_2$-CaO System. *Journal of Materials Chemistry*, **3**, 541-546. https://doi.org/10.1039/JM9930300541

[20] Kim, D.-G., Van Hoek, C., Liebske, C., Van Der Laan, S., Hudon, P. and Jung, I.-H. (2012) Phase Diagram Study of the CaO-CaF$_2$ System. *ISIJ International*, **52**, 1945-1950. https://doi.org/10.2355/isijinternational.52.1945

[21] Kim, D.-G., Van Ende, M.-A., Van Hoek, C., Liebske, C., Van Der Laan, S. and Jung, I.-H. (2012) A Critical Evaluation and Thermodynamic Optimization of the CaO-CaF$_2$ System. *Metallurgical and Materials Transactions B*, **43**, 1315-1325. https://doi.org/10.1007/s11663-012-9733-4

[22] Mukerji, J. (1965) Phase Equilibrium Diagram CaO-CaF$_2$-2CaO.SiO$_2$. *Journal of the American Ceramic Society*, **48**, 210-213. https://doi.org/10.1111/j.1151-2916.1965.tb14715.x

[23] Chatterjee, A.K. and Zhmoidin, G.I. (1972) The Phase Equilibrium Diagram of the System CaO-Al$_2$O$_3$-CaF$_2$. *Journal of Materials Science*, **7**, 93-97. https://doi.org/10.1007/BF00549555

[24] Ries, R. and Schwerdtfeger, K. (1980) Contribution to the Phase Diagram CaF$_2$-CaO-Al$_2$O$_3$. *Archiv für das Eisenhüttenwesen*, **51**, 123-129. https://doi.org/10.1002/srin.198004815

[25] Davies, M.W. and Wright, F.A. (1970) Viscosity of Calcium Fluoride-Based Slags. *Chemistry & Industry*, **11**, 359-363.

[26] Baak, T. (1954) The System CaO-CaF$_2$. *Acta Chemica Scandinavica*, **8**, 1727. https://doi.org/10.3891/acta.chem.scand.08-1727

[27] Bale, C.W., Chartrand, P., Degterov, S.A., Eriksson, G., Hack, K., Ben Mahfoud, R., Melançon, J., Pelton, A.D. and Petersen, S. (2002) FactSage Thermochemical Software and Databases. *Calphad*, **26**, 189-228. https://doi.org/10.1016/S0364-5916(02)00035-4

[28] Bale, C.W., Bélisle, E., Chartrand, P., Decterov, S.A., Eriksson, G., Hack, K., Jung, I.-H., Kang, Y.-B., Melançon, J., Pelton, A.D., Robelin, C. and Petersen, S. (2009) FactSage Thermochemical Software and Databases—Recent Developments. *Calphad*, **33**, 295-311. https://doi.org/10.1016/j.calphad.2008.09.009

[29] Höhne, G.W.H., Hemminger, W. and Flammersheim, H.-J. (1996) Differential Scanning Calorimetry: An Introduction for Practitioners. Springer, Berlin, Heidelberg. https://doi.org/10.1007/978-3-662-03302-9

[30] Tammann, G. (1903) Über die Ermittelung der Zusammensetzung chemischer Verbindungen ohne Hilfe der Analyse. *Zeitschrift für anorganische Chemie*, **37**, 303-313. https://doi.org/10.1002/zaac.19030370121

[31] Guenet, J.M. (1996) Contributions of Phase Diagrams to the Understanding of Organized Polymer-Solvent Systems. *Thermochimica Acta*, **284**, 67-83. https://doi.org/10.1016/0040-6031(96)02892-4

[32] Rycerz, L. (2013) Practical Remarks Concerning Phase Diagrams Determination on the Basis of Differential Scanning Calorimetry Measurements. *Journal of Thermal Analysis and Calorimetry*, **113**, 231-238. https://doi.org/10.1007/s10973-013-3097-0

[33] Sano, N., Tsukihashi, F. and Tagaya, A. (1991) Thermodynamics of Phosphorus in CaO-CaF_2-SiO_2 and CaO-CaF_2-$CaCl_2$ Melts Saturated with CaO. *ISIJ International*, **31**, 1345-1347. https://doi.org/10.2355/isijinternational.31.1345